JOURNAL OF GEOPHYSICAL RESEARCH, VOL. 101, NO. D14, PAGES 19,465-19,481, AUGUST 27, 1996

Effect of dry-season biomass burning on Amazon basin aerosol concentrations and optical properties, 1992-1994

B. N. Holben, [1] A. Setzer, [2] T. F. Eck, [3] A.Pereira, [2] and I. Slutsker[4]

Abstract. Aerosol concentrations and properties have been derived from a network of ground-based Sun-sky radiometer measurements in Brazil's Amazon basin region since 1992. The measurements characterize the background aerosol environment and aerosol emissions from biomass burning at eight selected sites. The duration and frequency of the measurements provide the foundation of an aerosol climatology based on direct sun measurements of aerosol optical thickness and retrievals of size distribution from solar aureole measurements. The aerosol optical thickness measurements clearly illustrate that for sites located within regions of biomass burning the duration of smoke above background levels often exceeds 2 months and frequently at levels an order of magnitude above background. The aerosol optical thickness range during preburning conditions was 0.11 to 0.27 at 440 nm. Under these conditions, stratospheric aerosols from Pinatubo constituted a significant part of the signal in 1993 but were about 50% less in 1994. During the burning season, smoke elevated the aerosol optical thickness above 1.0 for seasonally averaged values measured at 440 nm at sites located in active source regions in Mato Grosso, Rondonia, and Tocantins states. The measurement sites are located in the cerrado and forest conversion areas. Analysis of the size distribution of the particles indicated that the increase in aerosol optical thickness was associated with an increase of an accumulation and coarse particle modes. The asymmetry factor "g", computed from the phase function, showed considerable spectral dependence between the preburning and burning seasonal phases. The 1020-nm channel was reduced from 0.66 to ~0.53, while at 440 nm little seasonal phase variation was noted. Conditions of burning were sufficiently strong that the atmospheric conditions associated with the climatological definition of a dry season was subdivided into (1) preburning, (2) transition to burning, (3) burning, and (4) transition to wet season phases for most sites. Averages and frequency distributions were used to characterize each seasonal phase by site. Changes in total column water vapor amount, also retrieved from direct sun measurements, did not have an apparent effect on the optical properties of the aerosols.

1. Introduction

The Amazon basin is a 5 x 10^6 km^2 region of primary forest interspersed with cerrado (savanna) situated on flood plains, plateaus, and mountains that are a significant source of aerosols, gases, and water vapor to the global atmosphere [*Harriss et al.*, 1990]. Tropical forest regions are a principal source of biogenic aerosols [*Cachier et al.*, 1985] and some measurements of these have been reported [*Lawson and Winchester*, 1979; *Artaxo and Orsini*, 1986; *Artaxo et al.*, 1988, 1990, 1993, 1994].

Of more recent concern, the tropical forests have become a source of carbonaceous aerosols from biomass burning and when combined with savanna regions may represent about 80% of the total global carbonaceous aerosol [*Crutzen and Andreae*, 1990]. Savanna and cerrado ecosystems have evolved with natural wildfires, but the advent of mechanized clearing practices and the resource requirements of a growing population have rapidly expanded anthropogenic biomass burning, particularly in Brazil. This is shown as an increase in deforestation from 1978 to 1988 in Brazil's "Legal Amazon" from ~ 2 to ~6% in a decade [*Skole and Tucker*, 1993]. Fires and emissions from biomass burning have been well documented in Brazil in a variety of ways. *Setzer and Pereira* [1991] have monitored the number of fires in Brazil with the National Oceanic and Atmospheric Administration's (NOAA) advanced very high resolution radiometer thermal bands since 1987. Their studies show the number of fires in the Amazon region is generally increasing but vary from year to year, depending on meteorology and changing economic conditions. The primary fire season is during most of August and September with about 300,000 fires seasonally being typical [*Setzer and Pereira*, 1991]. *Prins and Menzel* [1992, 1994] have used the Geostationary Operational Environmental Satellite (GOES) Visible Infrared Spin Scan Radiometer (VISSR) Atmospheric Sounder (VAS) *Artaxo et al.* [1994] have measured in situ ground-level aerosol size distributions and mass concentration for varying periods of time at a cerrado site, a forest site with biomass burning, and a background forest site all in Brazil. Their results clearly show a 5 to 8 times increase in aerosol mass concentration during the burning season of August and September.

Aerosol concentrations and properties contribute significantly to climate radiative forcing. *Hansen and Lacis* [1990, p. 718] have stated that "Aerosols are the source of our greatest uncertainty about climate forcing. Tropospheric aerosols are difficult to monitor because of their spatial inhomogeneity, but they are a crucial variable because of the

[1] NASA/Goddard Space Flight Center, Greenbelt, Maryland.
[2] Instituto de Pesquisas Espaciais, Sao José dos Campos, SaoPaulo, Brazil.
[3] Hughes STX Corporation, NASA/Goddard Space Flight Center, Greenbelt, Maryland.
[4] Science Systems and Applications, Inc., NASA/Goddard Space Flight Center, Greenbelt, Maryland

Paper number 96JD01114.
0148-0227/96/96JD-01114$09.00

strong anthropogenic influence on their amount." Additionally, modeling by *Charlson et al.* [1992] and *Penner et al.* [1992, 1994] suggests that the direct and indirect radiative effects of sulfate and other aerosols in the troposphere, including those from biomass burning, may be sufficient on a global basis to offset the radiative effects of increases in "greenhouse" gases. *Penner et al.* [1994] proposed that synoptic-to-global scale observations be made of the radiation budget as well as both the composition of the aerosol and uncertainty of the interactions with water vapor. Quantitative measurements are relatively sparse, discontinuous, and more likely found in developed regions of the world. *Crutzen and Andreae* [1990] estimated that 80% of the aerosol emissions from biomass burning originate in the poorly monitored tropics thus exacerbating our ability to understand their influence on climate forcing, remote sensing, ecosystem dynamics, and health.

Beginning in 1992, an effort was mounted to measure aerosol concentrations and properties from biomass burning during the southern Amazon dry season and to a limited extent part of the wet season. Following is an assessment of the data collected to date, emphasizing the temporal characterization of the spectral aerosol optical thickness, size distribution, and precipitable water for the eight measurement sites. In a few cases the vertical profile has been characterized as well as the spatial variability of the aerosols around the primary measurement sites.

2. Spectral Scanning Radiometer Measurements

2.1. Instrument Description

A monitoring program to measure aerosol concentrations and properties from biomass burning was begun in 1992 using automatic remote recording Sun- and sky-scanning spectral radiometers [*Holben et al.*, 1996]. These stations, located in regions of biomass burning in both the cerrado and forested areas of Brazil, were fully operational in 1993 and 1994. Sites were chosen to capture the southerly transport of aerosols out of the Amazon basin and to satisfy logistical constraints (Figure 1). The network of eight Sun-sky scanning spectral radiometers measured aerosol concentrations and properties in Brazil's Amazon basin during the June through October dry season in 1993 and again in 1994. Direct Sun measurements at 340, 440, 670, 870, 940, and 1020 nm were automatically made every 15 min, and sky radiance measurements were made hourly weather permitting. The data are transmitted via the NOAA Data Collection System geostationary satellite link to Wallops Island, Virginia, for near real-time processing into spectral aerosol optical thickness (AOT), wavelength exponent (alpha), and precipitable water (cm) [*Holben et al.*, 1996].

The sky radiance almucantar (measurements in a plane with a fixed view zenith angle that includes the Sun) and principal plane (measurements in a plane with a fixed view azimuth angle that includes the sun) measurements are made hourly throughout the day at small angles through the solar aureole and increasingly larger angles as the scattering angle increases. These data are inverted into phase function, size distribution, and aerosol optical thickness [*Nakajima et al.*, 1983; *Nakajima et al.*, 1986] using the first 40 degrees from the solar disk. The inversion scheme continues to be developed [*Nakajima et al.*, 1996], but sensitivity studies show that size distribution retrievals are reasonable between 0.1 and 4 mm [*Kaufman et al.*, 1992; *Remer et al.*, 1995].

2.2. Site Descriptions

The sites were chosen to represent regional aerosol conditions free from local sources of industrial or urban aerosols to capture the southerly transport of aerosols out of the Amazon basin and to meet the logistical constraints routine for instrument maintenance and security. The data presented here were collected at three cerrado sites where burning is historically a natural part of the landscape processes but is augmented by increased agricultural burning and presumably advection from forest burning. Four diverse forest sites were monitored in the eastern and southern Amazon basin. Burning at these sites is a recent phenomenon of the forest conversion process. All cerrado sites have a dry season, extending on average from May through September, and forested sites have a slightly shorter season [*Nimer*, 1989].

Porto Nacional (latitude = 10°S, longitude = 48°W), located on the eastern side of the Amazon basin, is on the Tocantins River between Brasilia and Belem. The elevation is the lowest of the cerrado sites (200 m), resulting in warmer daytime temperatures and a more arid environment than the other sites. Brasilia (latitude = 16°S, longitude = 49°W), on the southern watershed boundary of the Amazon River system, is situated at an elevation of 1000 m on the Brazilian central plateau. Rare frosts kill herbaceous vegetation, resulting in increased levels of dry fuel loading and subsequent large natural fires. Much of the natural vegetation has been removed for agricultural cultivation, and these fields are routinely burned. Cuiaba (latitude = 16°S, longitude = 55°W), also located on the southern border of the Amazon watershed, is about 500 km west of Brasilia. It also is in a cerrado region with agricultural cultivation and is presumably downwind of intense forest burning to the north.

Five forest sites were monitored between 1993 and 1994. Alta Floresta (latitude = 10°S, longitude = 55°W), ~600 km north of Cuiaba, is located in a seasonal forest and has been the site of intense biomass burning since 1974, when the town was founded. Primary forest fires have given way to secondary maintenance fires as the primary source of emissions in the region. Alta Floresta is now about 30 km from most sources of primary forest conversion. To the west, Jamari and Ji-Parana in the state of Rondonia were sites monitored in 1993 and 1994, respectively. Jamari (latitude = 9°S, longitude = 62°W) was located in the seasonal forest about 40 km from the nearest burning sites. This region has the highest proportion of primary forest burned relative to the other instrumented sites. Ji-Parana [latitude = 12°S, longitude = 60°W) is located in the heart of the highway BR364 colonization corridor. Burning in the Ji-Parana region is primarily from secondary growth and grass fires. The Tucurui site (latitude = 4°S, longitude = 48°W) at the Tucantins Dam is operated in cooperation with Electro Norte. It is on the east side of the Amazon basin about 500 km north of Porto Nacional. The region has seen significant deforestation but that seems to be on the decline. The last station, Santarem (latitude = 1°S, longitude = 55°W), is located on the main Amazon in a region of very low biomass burning and is downwind of undisturbed forests. This site can be considered to be approaching background conditions.

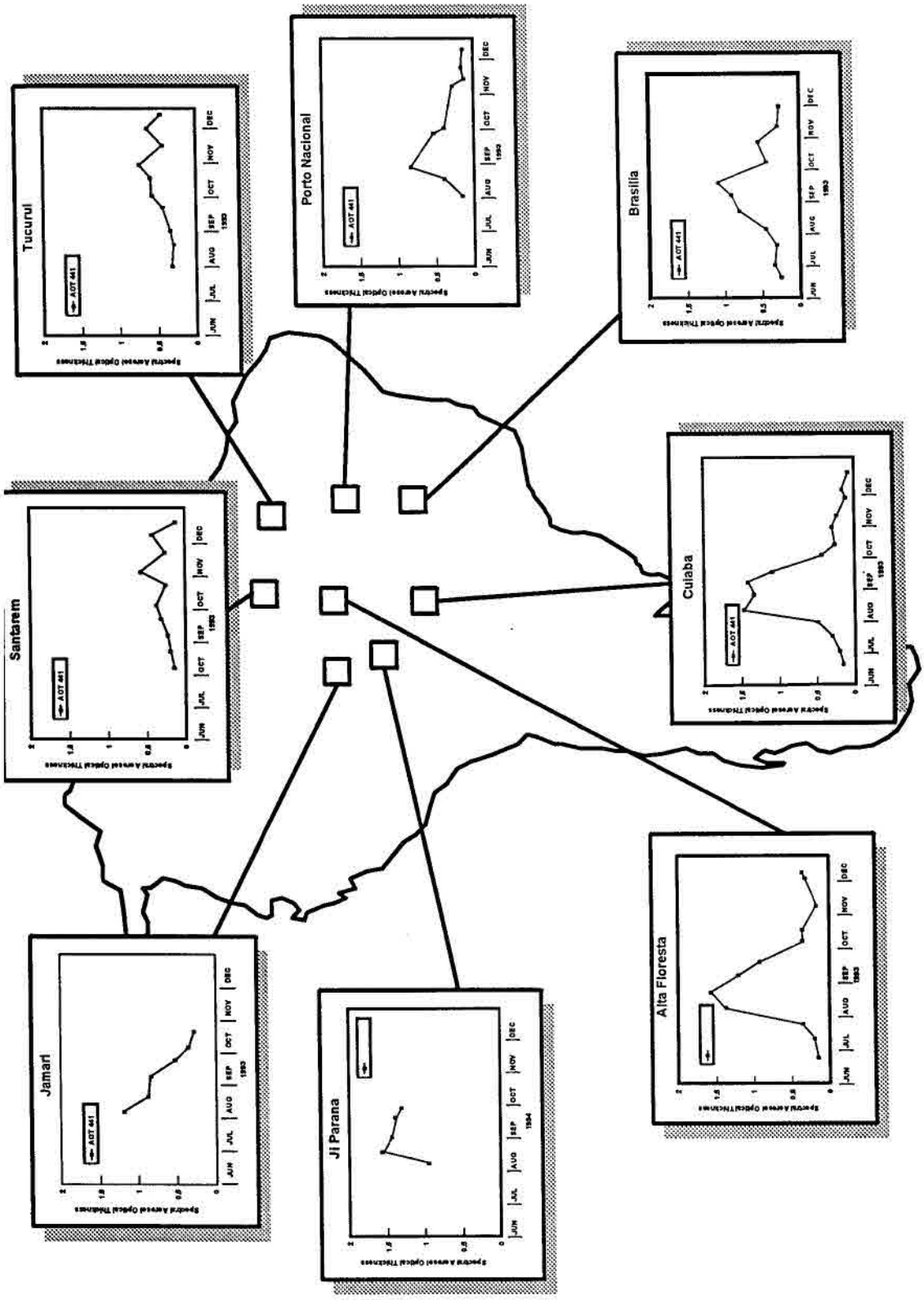

Figure 1. The aerosol optical thickness measured at 440 nm (AOT_{440}) averaged and plotted against date clearly shows the elevated levels of aerosols to be in the southern and eastern Amazon. This corresponds to the biomass burning activities in those regions.

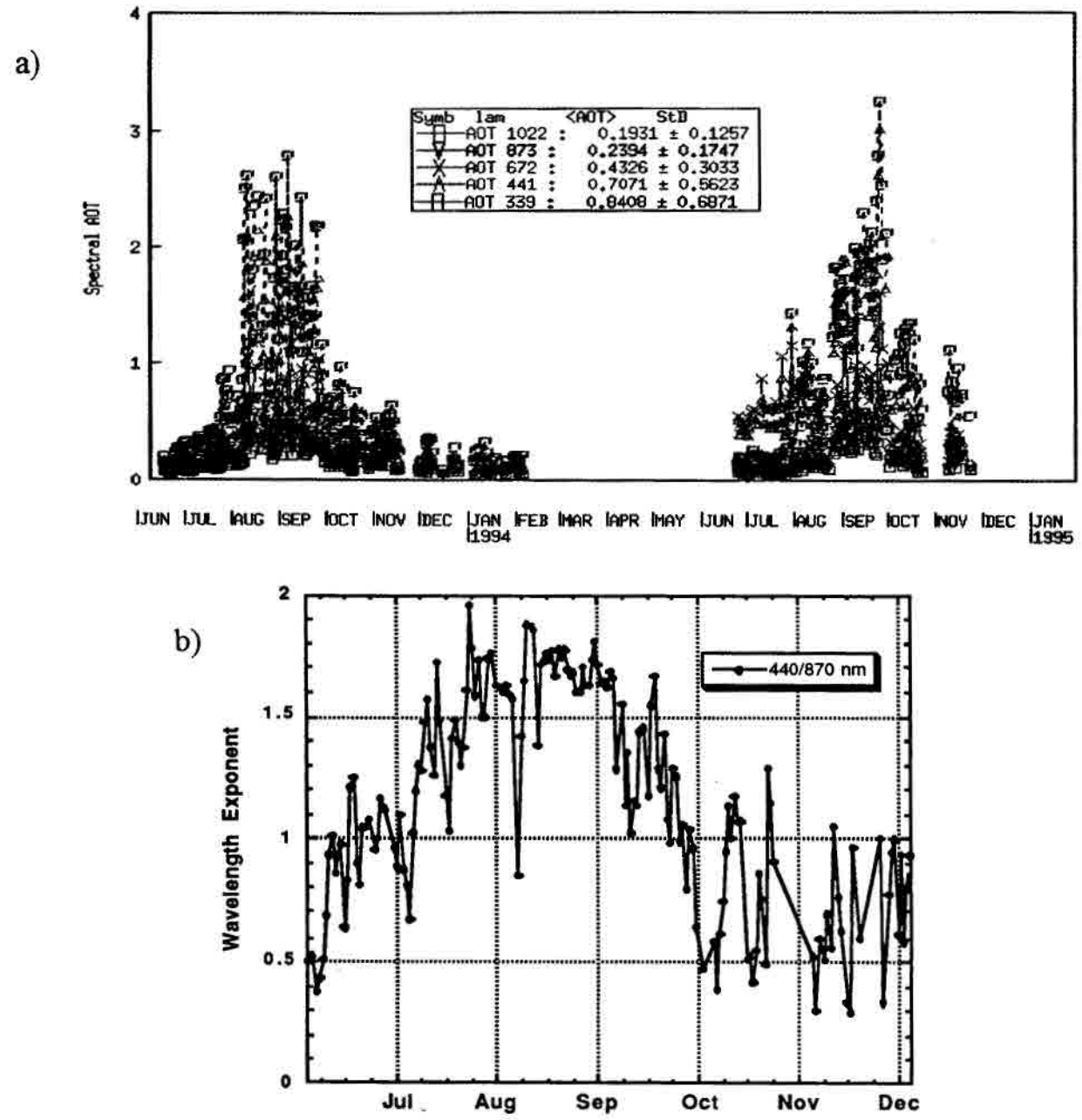

Plate 1. (a) Time dependent plots of the aerosol optical thickness during 1993 and 1994 in Cuiaba Brazil clearly show a massive infusion of aerosols into the atmosphere during August and September. (Note the 440 and 670 channels were not well characterized during July of 1994.) (b) The Ångstrom wavelength exponent for the 440/870 AOT ratio for 1993 , and (c) precipitable water in centimeters (1993) also show significant dynamics during the dry season.

2.3. Seasonal Measurements

Most of the Amazon basin is climatologically distinguished by a wet and dry season [*Nimer*, 1989]. However, with respect to aerosols, the dry season is clearly marked by nonburning and burning season phases for all sites along the southern and eastern forest margin; the duration of each varies by location and is caused by intraseasonal variations in weather patterns. The data from the Sun/sky spectral radiometer network clearly show the profound influence of biomass burning on the aerosol regime during the burning season (Figure 1). For all sites but Santarem and Tucurui, August and September show very heavy aerosol loading followed by a sharp decrease in October and the onset of the rains and the wet season. Prior to the burning season, the dry season optical depths were universally low for all measured sites thus representing background conditions that likely prevailed prior to major anthropogenic influences. A dramatic illustration of this is from Cuiaba in the cerrado region. Beginning in June 1993, AOT measurements were made through February 1994 which incorporated most of the dry season and several months of the wet season (Plate 1a). Two features stand out. First, there is a very high density of

c)

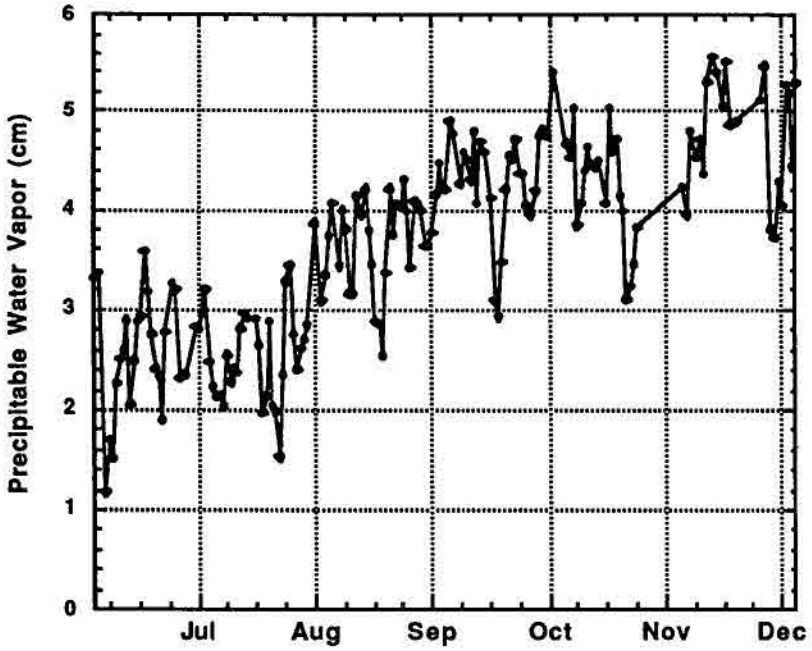

Plate 1. (continued)

a)

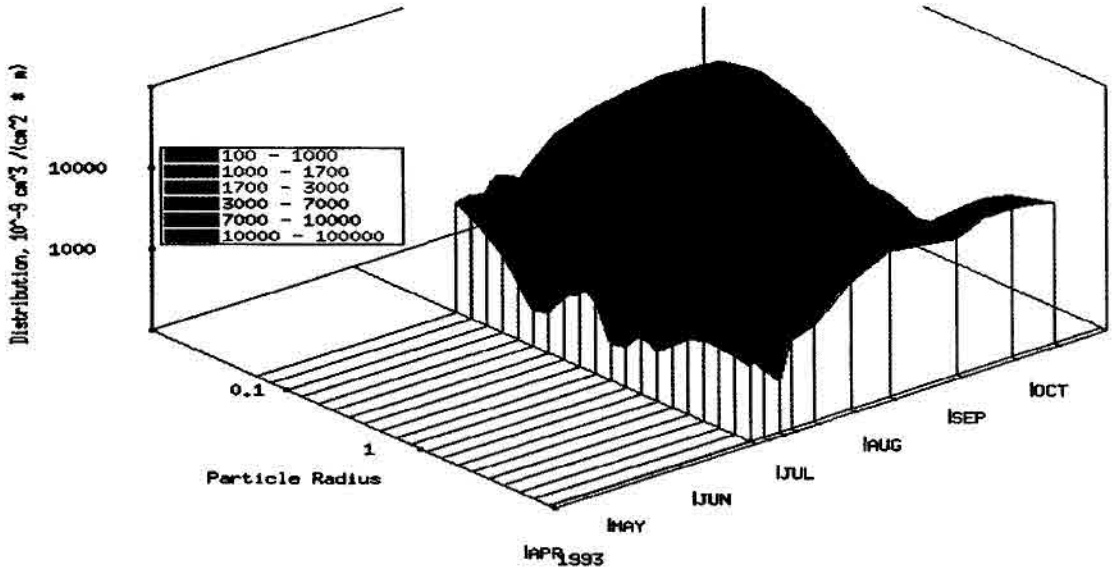

b)

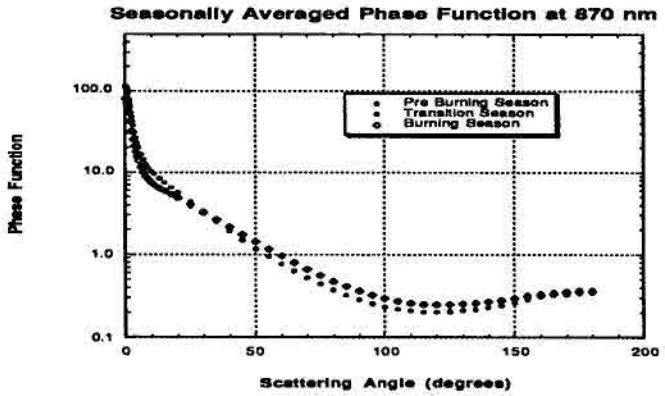

Plate 2. The almucantar radiance data were inverted to averaged aerosol size distributions and phase functions. (a) The time-dependent plot of the size distribution and (b) the phase function averaged for the clear, transition, and smoke seasons. Note the size distribution has peak values in the accumulation and coarse particle modes during the peak burning season of September.

Table 1. Mean Measurement Conditions for All Sites During the Aerosol Optical Depth Seasonal Phases

	λ, nm	Preburn	Transition to Burn	Burning	Transition to Wet	Wet
			Cuiaba 1993			
	870	0.09±0.02	0.15±0.04	0.41±0.13	0.15±0.05	0.11±0.04
	440	0.18±0.06	0.38±0.15	1.32±0.46	0.37±0.15	0.25±0.08
	alpha	0.95±0.23	1.31±0.25	1.71±0.12	1.25±0.28	1.10±0.17
Duration, days		>35	21	50	~30	>90
	Pw, cm	2.6±0.5	2.4±0.4	3.5±0.7	4.0±0.6	4.5±0.5
			Cuiaba 1994			
	870	0.07 ±0.02	0.20±0.08	0.45±0.15	ND	ND
	440	ND	ND	1.39±0.51	ND	ND
	alpha			1.61±0.17		
Duration, days		>30	25	30	ND	ND
	Pw, cm	ND	ND	3.4±0.6	ND	ND
			Alta Floresta 1993			
	870	0.10 ±0.02	0.15±0.06	0.42±0.15	0.19±0.05	0.15±0.05
	440	0.19±0.06	0.42±0.27	1.34±0.54	0.44±0.14	0.35±0.15
	alpha	0.86±0.27	1.35±0.31	1.69±0.16	1.23±0.22	1.16±0.26
Duration, days		60	~10	60	~30	
	Pw, cm	2.9±0.4	2.8±0.4	4.0±0.5	4.4±0.3	5.0±0.3
			Alta Floresta 1994			
	870	0.05±0.01	0.11±0.03	0.48±0.17	0.20±0.05	0.21±0.08
	440	0.22±0.07	0.60±0.16	1.73±0.62	0.54±0.16	0.41±0.18
	alpha	2.02±0.41	2.49±0.16	1.87±0.	1.48±0.25	0.93±0.23
Duration, days		>60	~15	>50	10	
	Pw, cm	2.8±0.3	2.8±0.6	3.8±1.0	4.4±0.4	6.3±0.4
			Santarem 1993			
	870	0.15±0.05	ND	ND	0.23±0.08	0.19±0.07
	440	0.27±0.09	ND	ND	0.44±0.17	0.37±0.17
	alpha	0.76±0.21	ND	ND	0.94±0.21	0.88±0.28
Duration, days		>35	ND	ND	~33	>45
	Pw, cm	5.3±1.0	ND	ND	5.8±0.9	6.3±0.4
			Jamari 1993			
	870	ND	ND	0.35±0.17	0.18±0.09	0.13±0.08
	440	ND	ND	1.17±0.58	0.40±0.18	0.23±0.15
	alpha	ND	ND	1.75±0.24	1.14±0.35	0.65±0.32
Duration,days		ND	ND	41	32	
	Pw, cm	ND	ND	4.3±0.6	4.7±0.4	5.1±0.7
			Ji-Parana 1994			
	870	ND	ND	0.37±0.14	ND	ND
	440	ND	ND	1.28±0.51	ND	ND
	alpha	ND	ND	1.81±0.20		
Duration,days		ND	ND	61	ND	ND
	Pw, cm	ND	ND	3.4±0.7	ND	ND
			Brasilia 1993			
	870	0.08±0.02	0.10±0.03	0.26±0.08	0.21±0.10	0.08±02
	440	0.11±0.02	0.18±0.07	0.76±0.24	0.49±0.28	0.15±0.06
	alpha	0.55±0.15	0.87±0.27	1.59±0.19	1.15±0.26	0.97±0.31
Duration , days		>7	42	40	44	>56
	Pw, cm	1.2±0.2	1.5±0.3	1.9±0.5	2.7±0.5	2.5±0.5
			Brasilia 1994			
	870	0.05±0.02	0.08±0.04	ND	ND	ND
	440	0.09±0.04	0.17±0.10	ND	ND	ND
	alpha	0.79±0.27	0.96±0.34	ND		
Duration , days		>73	>19	ND	ND	ND
	Pw, cm	1.7±0.4	1.4±0.3	ND	ND	ND

Table 1. (continued)

			Porto Nacional 1993			
	870	0.09±0.03	0.13±0.04	0.19±0.10	0.17±0.03	0.11±0.04
	440	0.17±0.08	0.18±0.05	0.55±0.39	0.41±0.11	0.15±0.07
	alpha	0.79±0.32	1.29±0.26	1.26±0.50	1.30±0.24	0.50±0.21
Duration , days		>18	14	28	8	>43
	Pw, cm	2.6±0.3	3.4±0.5	3.7±0.4	4.6±0.3	4.3±0.6
			Porto Nacional 1994			
	870	ND	0.26±0.28	0.28±0.20	0.20±0.07	ND
	440	ND	0.66±0.34	0.87±0.51	0.46±0.11	ND
	alpha	ND	1.57±0.67	1.78±0.53	1.27±0.41	ND
Duration , days		>22	17	23	14	ND
	Pw, cm	ND	2.8±0.8	3.1±0.7	4.2±0.6	ND
			Tucurui 1994			
	870	0.18±0.04	0.25±0.07	ND	0.29±11	ND
	440	0.35±0.09	0.52±0.24	ND	0.64±0.32	ND
	alpha	0.95±0.24	1.00±0.28	ND	1.09±0.27	
Duration , days		~60	~30	ND	~30	ND
	Pw, cm	4.2±0.4	4.4±0.4	ND	4.9±0.5	ND
			Tucurui 1993			
	870	0.15±0.05	0.20±0.07	0.31±0.16	0.41±0.25	ND
	440	0.28±0.07	0.44±0.16	0.78±0.55	1.14±0.79	ND
	alpha	0.98±0.17	1.14±0.23	1.25±0.30	1.34±0.30	ND
Duration , days		6	25	16	12	ND
	Pw, cm	4.1±0.3	4.2±0.3	4.3±0.4	4.1±0.4	ND

Pw, precipitable water; ND, no date.

measurements from June to early October (the dry season) and relatively few points from October to February (the wet season) because of the persistent cloud cover which prevents measurements from being taken.

The second feature of this record shows an order of magnitude increase in AOT beginning in late July and persisting until early October. This is the anthropogenic seasonality, caused by biomass burning in the region. The spectral optical thickness is used to compute the Ångstrom wavelength exponent (alpha) and is defined as

$$a=-\ln(AOT1/AOT2)/\ln(l_2/l_1). \quad (1)$$

Holben et al. [1991] and *Kaufman et al.* [1992] have shown the wavelength exponent to be sensitive to the rapid aging process of fresh smoke from fires in Brazil, estimating the effective geometric radius from 0.15 for smoke less than 10 min old to 0.20 for smoke more than a day old. Many other investigators have related the wavelength exponent to the mean particle size. The seasonal distribution of the wavelength exponent shows an increase in value coinciding with the burning season (Plate 1b), indicating that the proportion of particulate emissions is shifted toward smaller particles during the burning season. Precipitable water (Pw) is measured by the instrument which has a nominal absolute accuracy of ±0.3 cm [*R.N. Halthore et al.*, unpublished manuscript,1996]. The seasonal dependence for Cuiaba shows an increase in Pw through the dry season. September has Pw levels similar to the wet season, which is about 70% higher than the early burning season values (Plate 1c).

The size distributions were retrieved from inversion of the daily spectral almucantar measurements made between an optical airmass of 5 and 2. The seasonal plot clearly shows the increase of the accumulation and coarse particle modes which overwhelms the constant Pinatubo mode (centered near 0.5 mm) during August and September 1993 (Plate 2a). Further evidence of the influence of the anthropogenic emissions is shown by the difference in the retrieved phase function between the early dry season (preburning) and late dry season (burning) (Plate 2b).

These data indicate that the current aerosol climatology of the Amazon region should be partitioned beyond the simple climatological limits of the wet and dry season. For regions of active biomass burning, we have subdivided the dry season into a preburning season, a transition to burning season, a burning season, and a transition to wet season. These categories are relatively subjective in their boundaries; however, we have defined them by the magnitude and temporal variability of the average aerosol optical thickness at 440 nm (AOT_{440}). For example, the average AOT_{440} during the preburning season remained below 0.4 and has a standard deviation of less than 0.04. The transition to burning had an average AOT_{440} ranging between 0.4 and 1.0, the burning season greater than 1.0, the transition to wet again between 1.0 and 0.4, and the wet season less than 0.4. The lack of data in the wet and early preburning seasonal phases limits our ability to characterize these well; however, we assume the Amazon basin has few sources of anthropogenic aerosols during these periods and feel our limited measurements characterize the aerosol environment fairly well during that time.

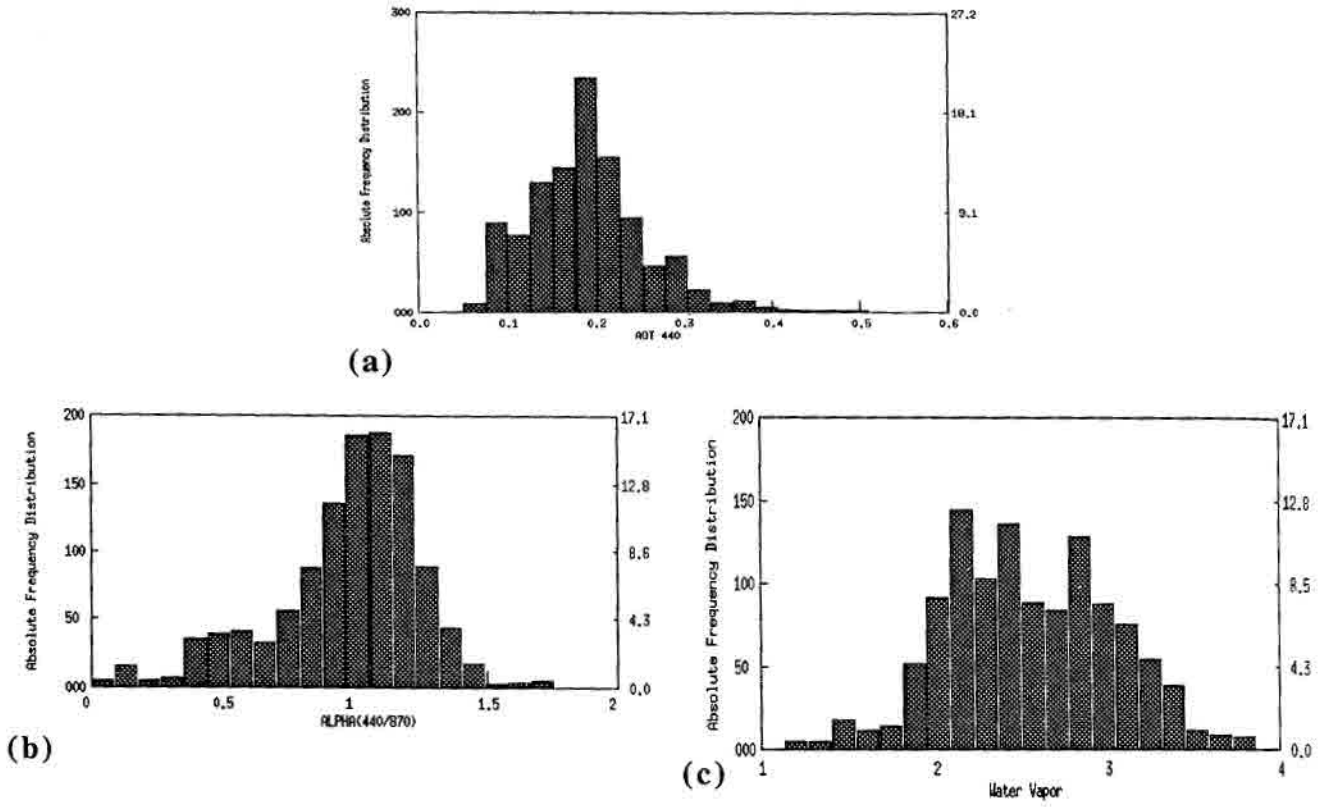

Figure 2. The frequency distribution of the (a) AOT_{440}, (b) Ångstrom wavelength exponent (440/870), and (c) precipitable water (cm) indicate the temporal stability of the aerosol environment during the preburning season.

The Brazilian Amazon basin covers approximately 5 x 10^6 Km^2. The sun photometer network is a point network of eight stations that were situated to monitor aerosol emissions from biomass burning within the context of the counterclockwise synoptic atmospheric circulation. These measurements cannot and were not intended to represent the emissions over the entire Amazon region but do characterize the optical properties of aerosols and give an indication of the magnitude, variability, and duration within the region surrounding each site. In the following sections, we will characterize the AOT, wavelength exponent, Pw, and size distribution for a cerrado site (Cuiaba), a forested site (Alta Floresta), and a nonburning region (Santarem) for each subseason. A spatial variability study will contrast the burning and preburning seasons. Statistics of the aerosol magnitudes and properties for each site are tabulated in Table 1. Finally, at sites where 2 years of data are available, 1993 and 1994 will be contrasted.

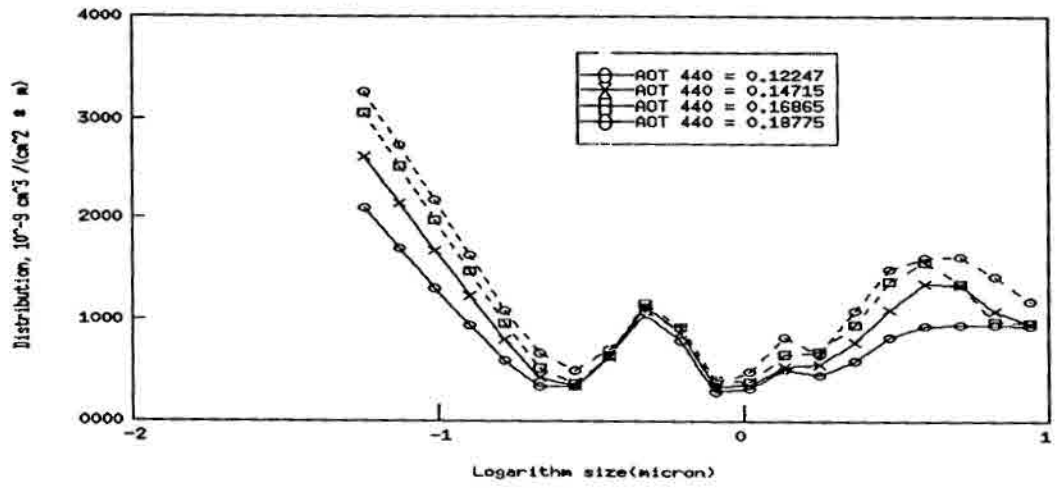

Figure 3. The size distribution during the preburning season showed a stable mode centered at 0.6 mm (Pinatubo stratospheric aerosols) and weak accumulation and coarse particle modes during 1993.

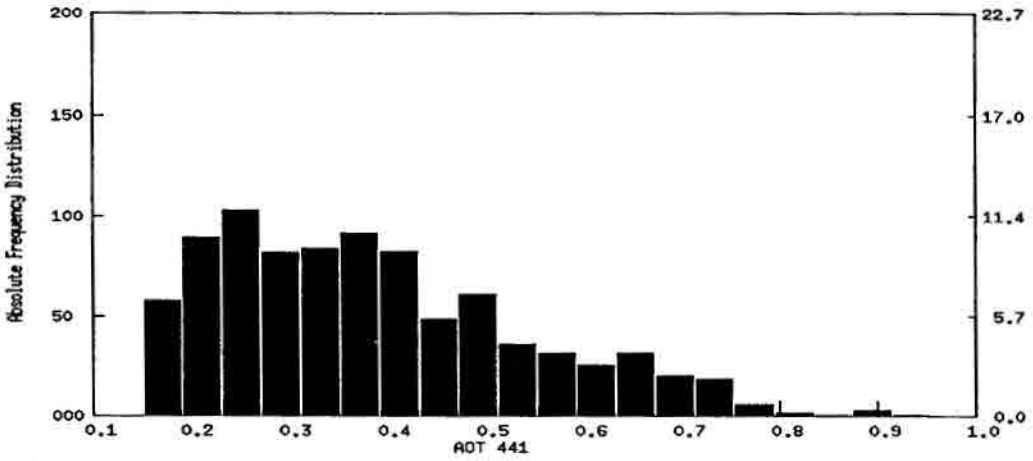

(a)

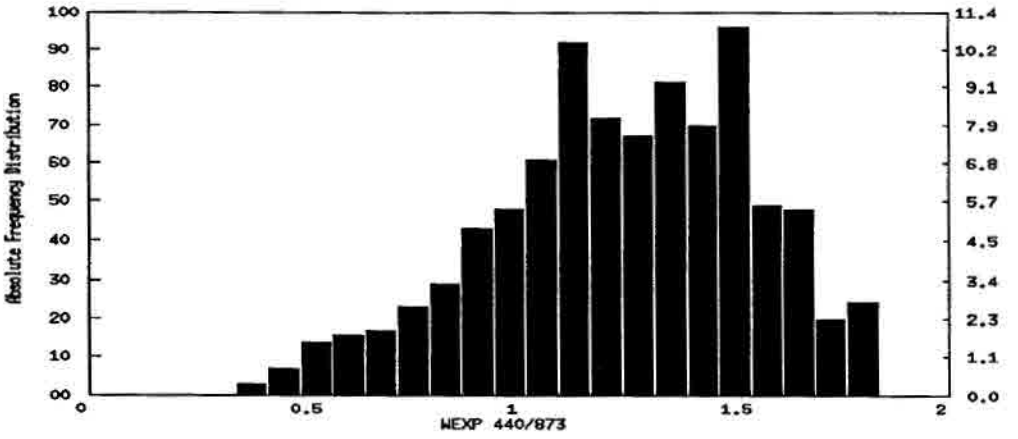

(b)

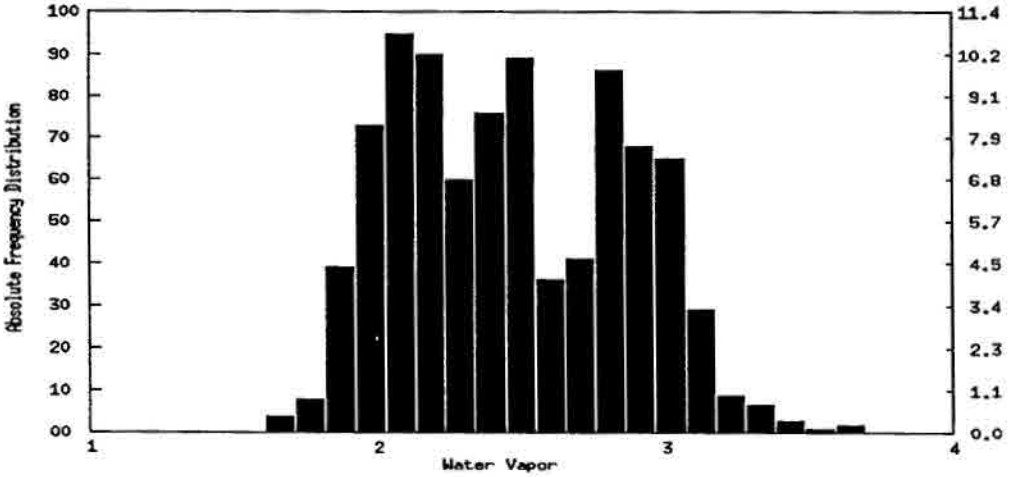

(c)

Figure 4. The (a) AOT_{440} frequency distribution, (b) Wavelength exponent, a, and (c) Pw are shown for the transition season in Cuiaba.

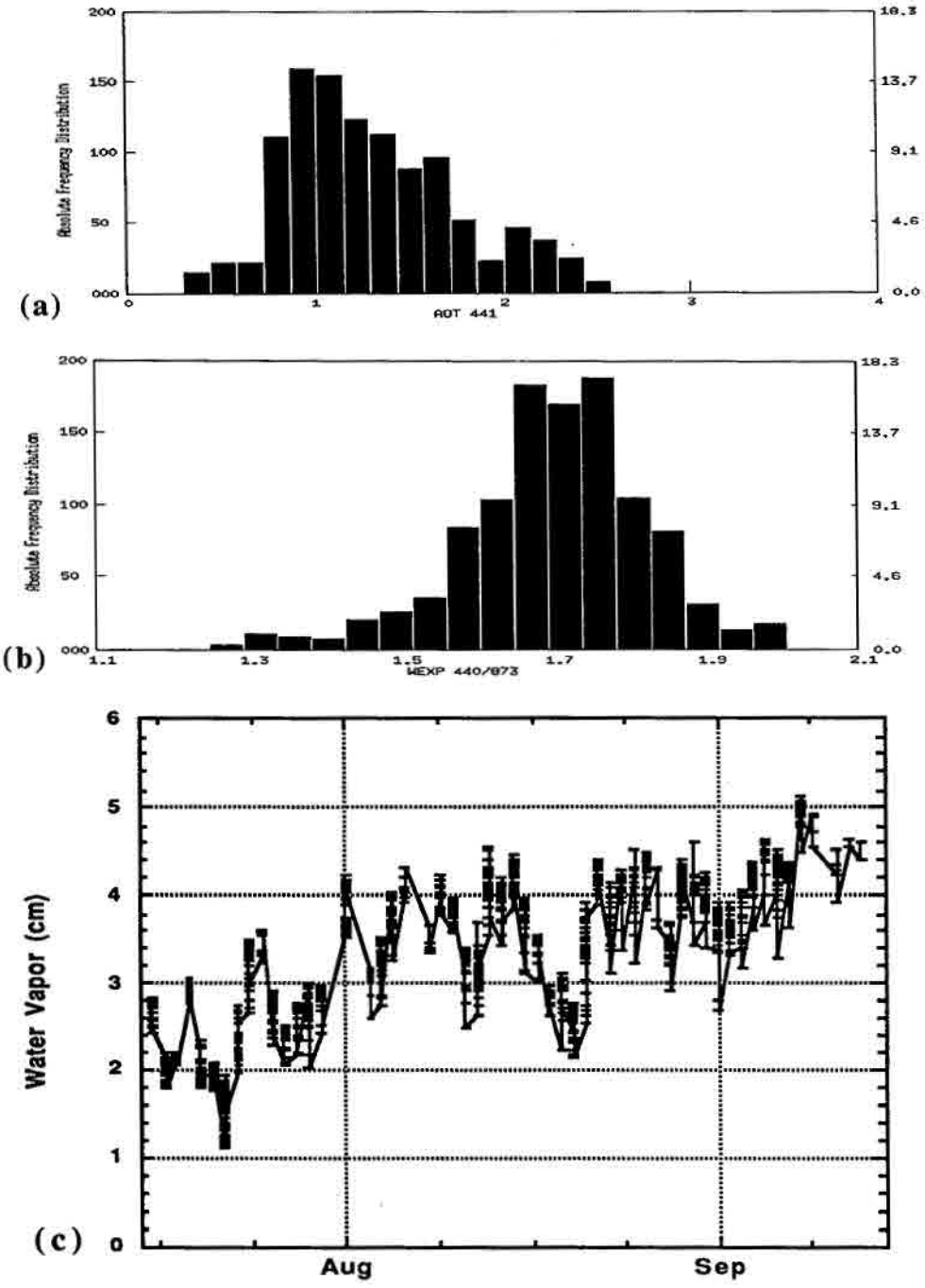

Figure 5. (a) The AOT_{440} frequency distributions of the burning season shows little variation when analyzed by morning and afternoon distributions. (b) The burning season frequency distribution of the Ångstrom wavelength exponent shows a slight bimodal distribution; the higher value likely represents a response to fresh smoke from afternoon fires. (c) The Pw during this period shows an increase from ~2.5 cm at the beginning of the burning period to ~4.0 cm near the end.

3. Cerrado Site: Cuiaba

3.1. Preburning Seasonal Phase

The preburning seasonal phase, as measured from June 9 to July 15, 1993, almost certainly began prior to our first measurements. The average aerosol optical thickness and standard deviation, was 0.18 (±0.06) at 440 nm and the Ångstrom wavelength exponent, a, was 0.95 (± 0.23) (Table 1). The frequency distribution of the AOT_{440}, a, and P_W illustrates the stability of the aerosol conditions and water vapor during this period (Figure 2). These values are relatively typical for all sites during preburning and could be considered background levels which, in part, were influenced by the stratospheric Pinatubo aerosols during this time [*Dutton*,

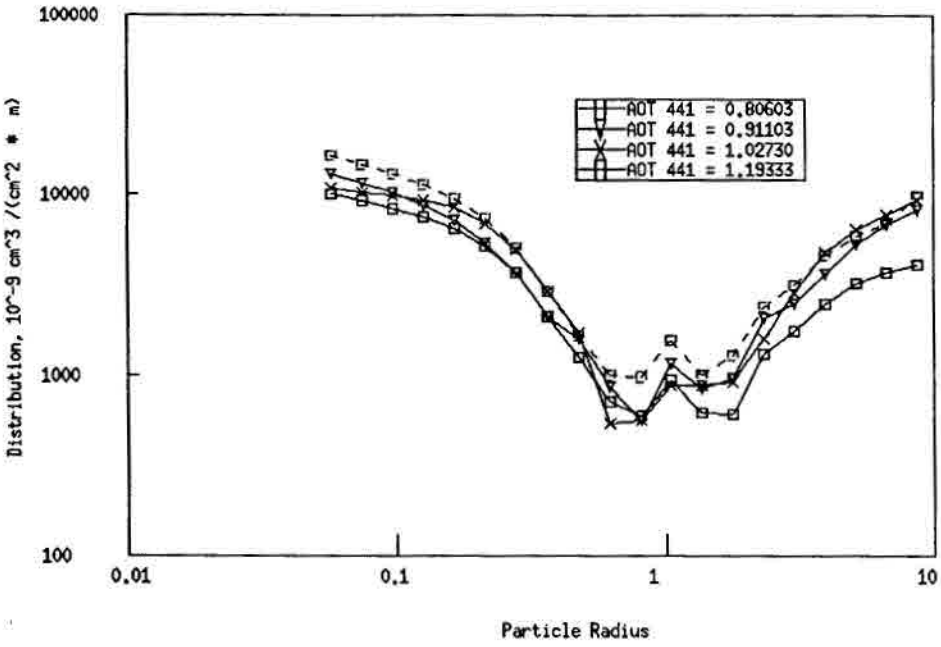

Figure 6. The size distribution during the burning season shows very large accumulation and coarse particle modes when compared to background conditions (Figure 5).

1994]. The Pinatubo aerosol optical depth at 525 nm for this time period was measured at midlatitude sites [*Rosen et al.*, 1994] to be ~0.035 at a northern hemisphere site and 0.07 at a southern hemisphere site. The volume size distribution from the almucantar data typically show a weak accumulation mode (representative for radii larger than 0.1 mm, [*Remer et al.*, 1995]), a Pinatubo mode centered at 0.6 mm, and a weak coarse particle mode to about 8 mm (Figure 3). During very clear conditions (AOT_{440} = 0.1), the dominant mode is that caused by the Pinatubo aerosols. (In 1994, the Pinatubo mode was reduced in magnitude by 50% compared to 1993.) Measurements extended for about 35 days at this level with very little diurnal variation and likely represent conditions in the dry season prior to our measurements. They are also similar to the few measurements obtained during the wet season and therefore are probably a good estimator of nonanthropogenic background conditions for the southern Amazon basin.

3.2. Transition to Burning Season

The transition to burning season is a subjective time interval, although conceptually it is rather easy to define. The transition occurs as a few agriculturists burn their fields prior to complete drying of the fuels in the region. A few fires emit a relatively small amount of aerosols into the atmosphere resulting in small increases in the AOT. Because there is not widespread burning, the AOT returns to nearbackground levels until a few more fires are begun a few days later. This cyclic pattern may continue for a few weeks. For Cuiaba in 1993, the transition season lasted from July 15 to August 6. The Ångstrom wavelength exponent (440/870) during this time oscillates between the background levels of 0.9 to burning conditions of 1.6 with a mean of 1.31 (0.25 s.d.) and the AOT oscillates between background levels 0.18 to 0.90 with a mean of 0.38 (0.15 s.d.). Precipitable water remained low and fairly constant during this period with the frequency distributed mainly between 2.0 and 3.0 cm with a mean of 2.4 cm (Figure 4).

3.3. Burning Season

During the nearly 2-month burning portion of the dry season, August 7 to September 27, the AOT_{440} averaged 1.32 (0.46 s.d.) with a wavelength exponent of 1.71 (0.12 s.d.), indicating the presence of a large population of small particles for the 2-month duration. AOT_{440} ranged from 0.40 to 2.80 for this time period, but the wavelength exponent varied from 1.28 to 1.98; the larger number suggests the presence of fresher smoke due to a higher proportion of fine to large particles (Figures 5a and 5b). Because most fires are ignited after local noon, a difference in the scattering and absorption properties would be expected between the fresh smoke in the afternoon and the aged smoke of the mornings. The difference between the morning and afternoon peak a frequency distributions shows only slight variations from 1.7 and 1.8 in the morning and afternoon, respectively, and the distributions are fairly broad and nearly identical. The AOT_{440} frequency distributions also do not show a clear increase from morning to afternoon. Both situations suggest that the scenario of local burning around Cuiaba is less important and that much of the smoke is probably advected from the surrounding regions.

Almucantar inversions at extremely high optical thicknesses were more difficult to obtain because of the inhomogenious distribution of the aerosols in the viewing scans of the instrument as well as the instability induced when inverting multiple scattered radiation. Almucantars taken during average aerosol loading were often unsuccessfully inverted. Those that were inverted showed size distributions with very large accumulation modes which nearly masked the Pinatubo mode (Figure 6). Typically, the accumulation mode was 20 times greater than background conditions and the coarse particle mode approximately an order of magnitude above background conditions.

Precipitable water during this time increased from less than 2 cm in early August to more than 4 cm in late September (Figure 5c). This would be expected to cause some variation of the aerosol properties either directly by condensation or absorption or indirectly through cloud processing. This also suggests that cloud interactions with aerosols is likely to be more prevalent during the latter part of the burning season and direct radiative forcing more significant during the early part of the burning season. Contrasting the wavelength exponent between the first 2 weeks and the last 2 weeks of the burning season, however, does not indicate a significant difference between the properties of the aerosols in Cuiaba.

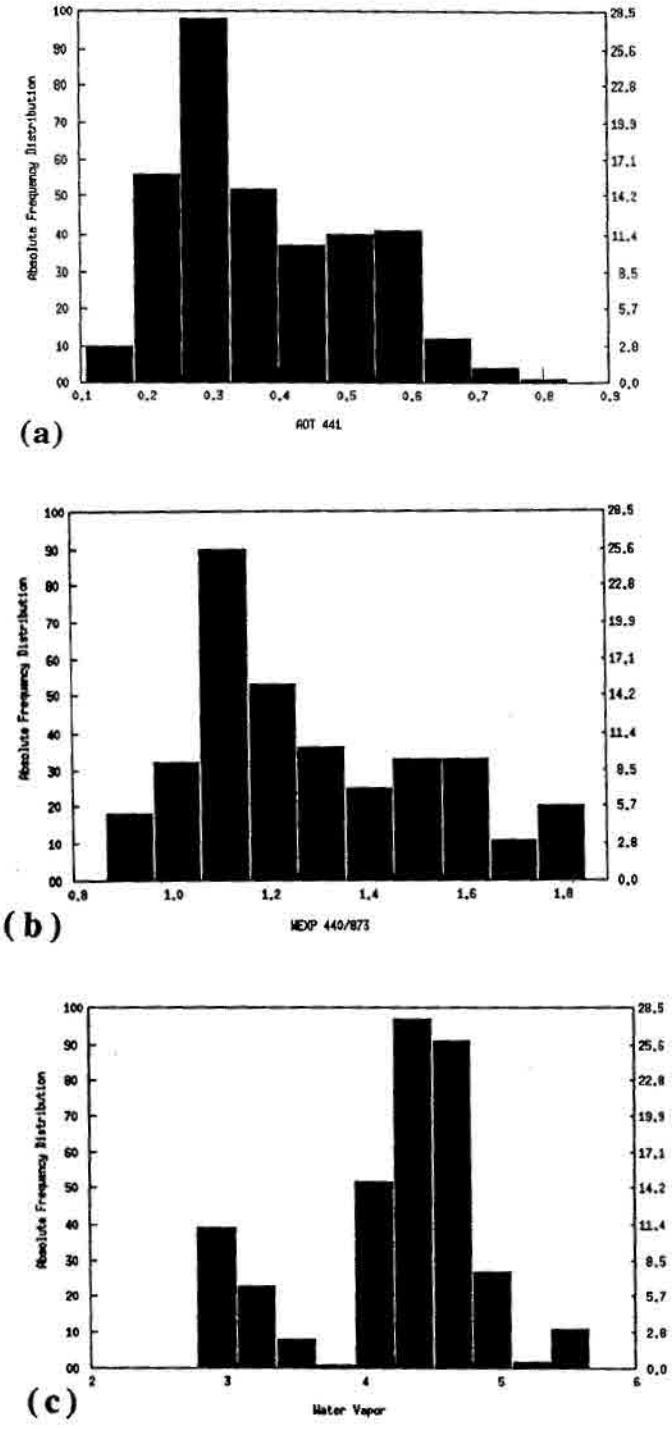

Figure 7. (a) The AOT_{440} frequency distribution for the transition to wet season and wet season combined indicates a relatively narrow peak at low optical thicknesses, as would be expected. (b) The wavelength exponent distribution indicates a shift toward smaller values from the burning season and (c) precipitable water is a bimodal distribution indicating that water vapor is in transition during this time.

3.4. Transition to Wet Season

The transition to the wet season lasted from September 27 to November 1 and the wet season began thereafter. Because of the paucity of data in both periods, the data were combined. The frequency distribution of the AOT_{440} is shifted toward small AOTs typical of background conditions. However, particulates from late season burning account for the larger AOTs (Figure 7a). This is substantiated by the Ångstrom wavelength exponent, which shows a wide distribution ranging from 0.9 for clear air to greater than 1.8 for smoke (Figure 7b). The distribution of Pw is bimodal (Figure 7c). The weaker mode (3 cm) is due to a few dry days during the transition, and the higher mode is more indicative of the wet season (4.7 cm). Few sky radiance data were taken during this time because of the increased presence of clouds, so a climatological analysis of the size distribution was not possible.

3.5. Comparison to 1994

In 1994, the magnitudes of the averaged AOTs during both the dry and burning seasons were very similar to 1993, but the duration was dramatically different for Cuiaba. For example, the transition to burning was essentially nonexistent in 1994, and the burning season began in late August and extended for approximately 30 days, compared to 50 days in 1993. The timing and duration of the Pw remained approximately the same. The authors have no ancillary data to explain this phenomena; however, it is suspected that regional meteorology played a significant role.

4. Forested Site

4.1. Alta Floresta

Aerosol properties at forest sites where burning occurred were similar to the cerrado; however, the Ångstrom wavelength exponent was more variable during the burning season, probably because of a greater influence of fresh smoke from local burning. An example of this is the Alta Floresta data record, where measurements began in June 1993 and ran through October. The data show a very clear preburning season (AOT_{440} = 0.19, a = 0.86) until the transition in mid-July. The burning season began in early August (AOT_{440} = 1.34, a = 1.69) with a duration of approximately 60 days (Table 1). Compared to Cuiaba and the cerrado sites, these data show more distinction between morning and afternoon conditions with an increase in AOT and Ångstrom wavelength exponent in the afternoon (Figure 8). However, considering the entire burning season, these differences amount to an increase of only a few percent and likely only become significant when individual cases are examined. The size distribution and phase function retrieved during this time also are very similar to the conditions in Cuiaba. The size distributions indicated a close relationship to the AOTs, that is, low AOTs showed weaker accumulation and coarse particle modes and are entirely consistent with measurements in the cerrado (Figures 9 and 5).

Considering the large magnitudes of the AOT during the burning season and the variability of the meteorological

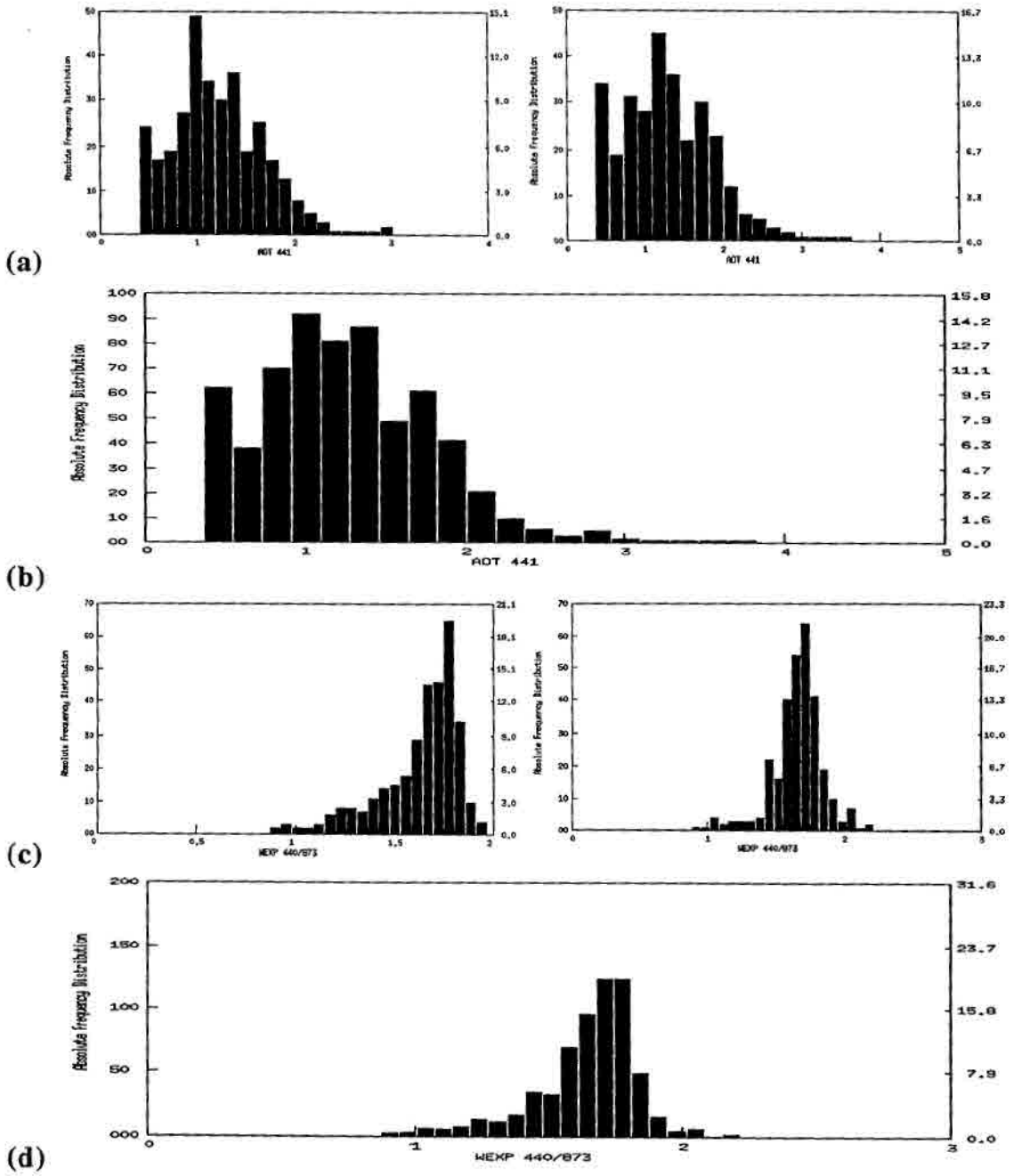

Figure 8. The frequency distributions for the Alta Floresta burning season (a) and (b) AOTs and (c) and (d) Ångstrom wavelength exponents were computed. (a) and (c) show the morning and afternoon distributions (left and right, respectively). (b) and (d) are the distributions combined for the full day. Note the slight shift to higher values in both the AOT and alpha distributions in the afternoon.

conditions, it is fairly remarkable that biomass burning emissions of this magnitude are repeated each year. The duration of the burning season was reduced in 1994 to 50 days, but there was a substantial increase in the magnitude of the AOT_{440} from 1.41 to 1.73 (Table 1).

4.2. Santarem

In contrast, Santarem had no significant anthropogenic aerosol loading. The AOT_{440} remained at background levels throughout the August and September dry season, the frequency distribution indicates that ~80% of the AOT_{440} is less than 0.2, and the wavelength exponent (0.88) is commensurate with what would be expected from combined background tropospheric and stratospheric Pinatubo aerosols [*Rosen et al.*, 1994; *Russell et al.*, 1993]. Regional burning was reported ~100 km to the south; however, the predominant wind direction is from the NE, where there are few sources of aerosols from biomass burning. There is a slight elevation of the AOT in November and December and a corresponding decrease in wavelength exponent. Since the Pw is the highest during this time thereby making the possibility of local or regional biomass burning sources unlikely, we suggest that the source is possibly Saharan dust transported across the Atlantic.

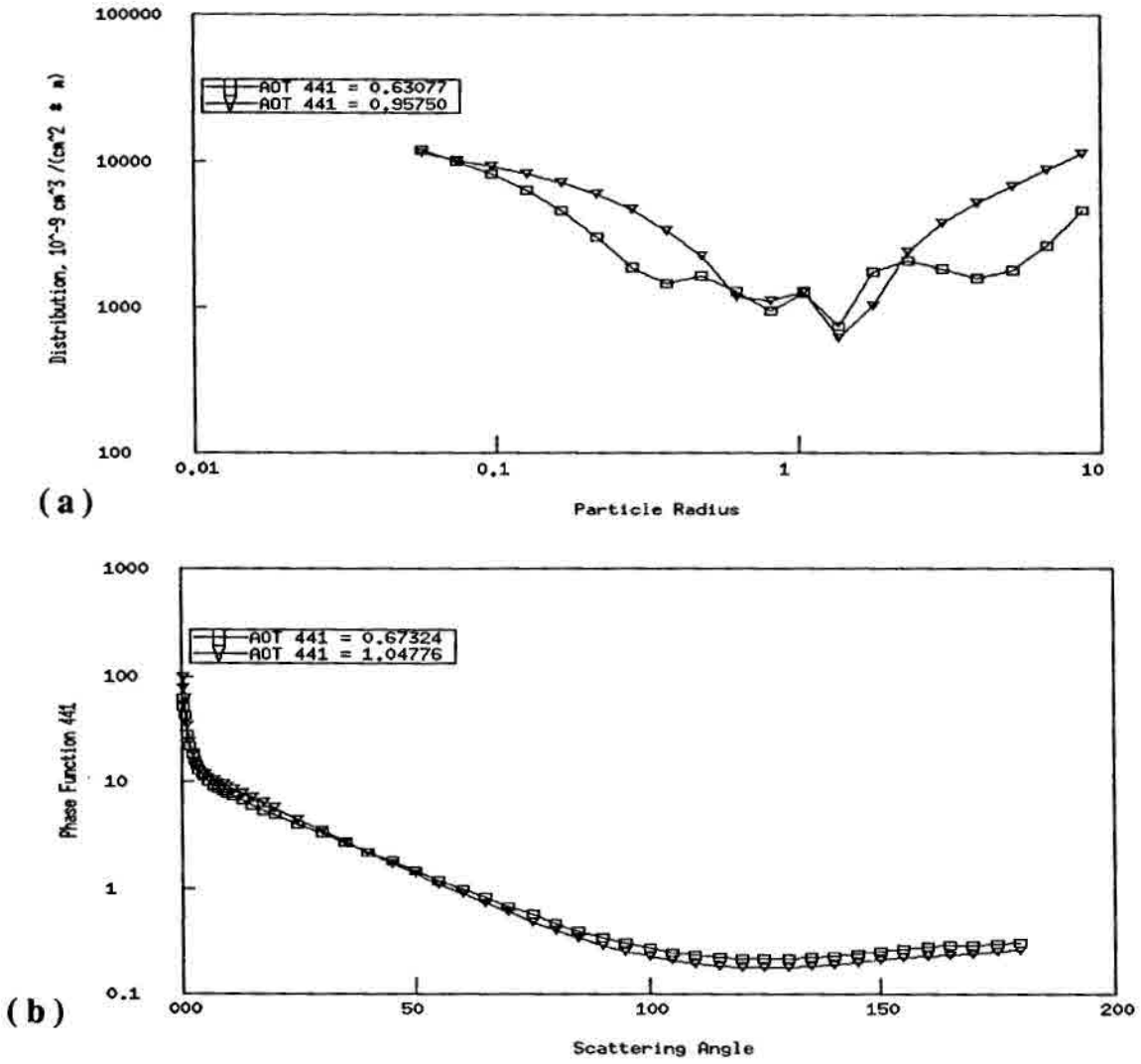

Figure 9. The (a) retrieved size distribution shows an increase in the accumulation and coarse particle modes with increasing AOT. Both the size distributions and (b) phase functions are similar to those retrieved from the cerrado.

5. Seasonal Temporal Variability

The variation of the AOT within the preburning subseason is very small and may be characterized by the simple standard deviation (Table 1). The burning season as well as the transition seasons show a great deal of variability in AOT (Table 1), and the standard deviation may not accurately represent the variation during this time for the following reason. During the burning season two situations are common: (1) well-mixed uniform smoke is advected from regional fires or (2) local fires cause great variability in the time-dependent aerosol concentration and properties.

The first case has two variants. In nonsource regions, aerosols are advected, creating aerosol fronts resulting in large changes in aerosol concentrations in short amounts of time. In Jamari, the frontal boundaries were observed to be very active, resulting in large temporal variations in AOT on the order of hours.

In the case of sites located within biomass burning regions, there are both diurnal variations in aerosol loading due to the diurnal cycle of the burning [*Prins and Menzel*, 1994] and advection of smoke from adjacent burning regions. As an example, the AOT_{440} in Porto Nacional over a period of 1 week, September 14-20, 1992, changed from a situation where there was a strong diurnal increase in AOT each day from fires starting in late morning to early afternoon. However, by the next morning the smoke aerosol had dissipated, and the cycle began again as fires were ignited. The meteorological conditions changed from September 17-20 where there were high AOTs all day with no distinct diurnal variation (Figure 10). This was the result of advection of smoke from biomass burning areas within the region. Figures 10b and 10c show that for the same AOT_{440} from 1.1 to 1.7, the Angstrom wavelength exponent was higher for the days which were dominated by smoke from local burning versus the smoke which was advected into the area on September 17-20 and thus more aged smoke. These data suggest smaller aerosol particles from the fresh smoke from fires burning on the same day versus the more aged and regionally advected smoke. Thus not only did the aerosol loading increase but the properties of the aerosols changed as well. This behavior was commonly observed in the data at most sites simply because they were located within burning regions away from local sources.

The second situation of intense local burning typically is represented by rapid oscillations in aerosol concentrations and

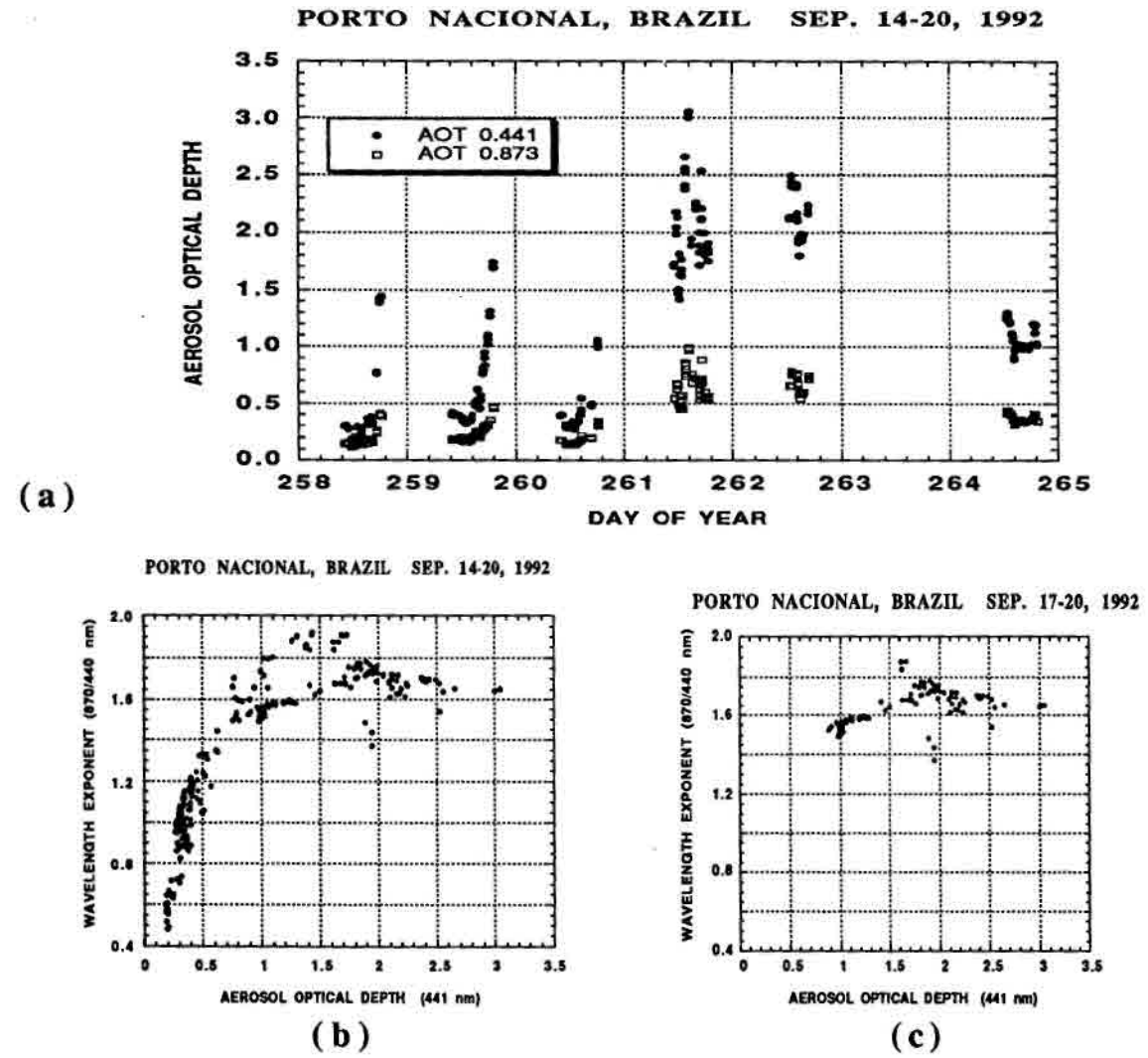

Figure 10. (a) Seven days of AOT measurements in Porto Nacional show two different regimes, one where local fires result in diurnal patterns of clear air and fresh smoke and the other where smoke is advected from adjacent regions. (b) The t_{440} versus a plot of this time series shows two distinct populations between the clean air (lower a) and the smoke contaminated air (higher a). This apparent advection is a common influence for many of the sites. (c) The same as (b) but for September 17-20, when the wavelength exponent was less despite very high AOTs.

properties due to smoke by plume remnants not yet mixed in the atmosphere. The period of these events often is of the order of minutes to a few hours. Data from a transect along highway BR364 in Rondonia illustrates this phenomenon (Plate 3). The stations which are farthest apart in this transect are only 90 km from each other. This typically occurs in the forested and forest-converted areas but is a less common feature of the aerosol environment than the regional events. Characterizing the aerosol properties from sky radiance measurements is nearly impossible during these events, whereas the spectral optical thickness is a reliable source of aerosol size distribution in these situations.

6. DISCUSSION

The concentrations and optical properties of aerosols in the Amazon basin have been shown to vary temporally and spatially because of emissions from anthropogenic biomass burning. Background aerosol concentrations ranged from 0.09 to 0.22 for AOT_{440} for all of the southern Amazon measurement sites (Table 1). Background levels were slightly modified in 1993 because of stratospheric Pinatubo aerosol loading particularly evident in the size distribution retrievals. However, by 1994 the volume distribution of the Pinatubo mode had been reduced by half. Because of lack of strong sources of anthropogenic aerosols, it is assumed that the majority of background aerosols are from natural biogenic sources.

The climatological dry season can last 5 months, but because of strong anthropogenic aerosol sources, we have defined four dry seasonal phases: background, transition to burning, burning, and transition to wet season. Significant aerosol emissions are present during all but the preburning season. The transition seasons are characterized by a cycle of clear to smoky conditions and the burning season by relatively constant and heavy aerosol loading. Angstrom wavelength exponent measurements of fresh smoke (a day or less old) typically range from 1.8 to 2.2 [*Kaufman et al.*, 1992;

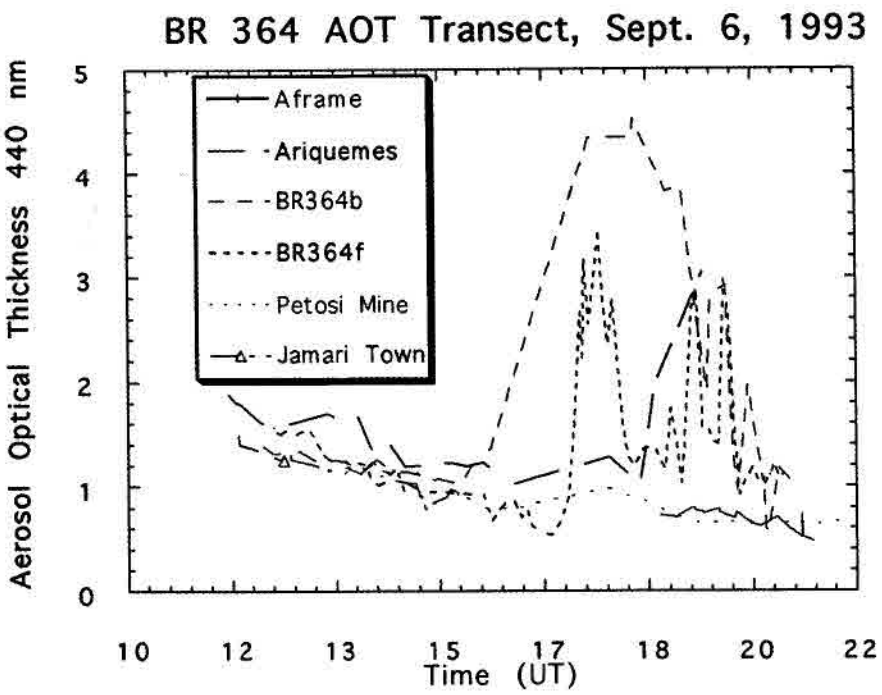

Plate 3. The AOT_{440} was measured throughout a day at sites various distances from local fires. Note that until noon (1600 UT) the AOT_{440} was very similar but diverted greatly in response to local fires. Petosi Mine and Aframe were located sufficiently far from active fires (~40 and 20 km, respectively) that no influence was observed. Ariquemes and the BR364 sites were in some cases within a few kilometers of local fires.

Holben et al., 1991]. The histograms of the wavelength exponent during the burning season suggests the smoke is typically aged more than 1 day. Cuiaba in 1993 and Alta Floresta in 1994 showed periods of 4 weeks or more of extremely high levels of aerosol loading from smoke advected from the surrounding region. The wavelength exponent during this time was typically 1.69 to 1.87, indicating that the smoke was aged (Table 1).

Inversion of the sky radiances were relatively few when the AOT_{440} exceeded 1.0 thus the size distribution and phase function retrievals are biased and may not fully represent aerosol properties during heavy loading events. Given these limitations, size distributions indicated a significant Pinatubo mode in 1993 centered at 0.6 mm that diminished by one half in 1994. As the burning season advanced, the accumulation and coarse particle modes increased, overwhelming the Pinatubo signal. In like manner, the retrieved phase function and asymmetry factor changed as the burning season advanced. For example, typical asymmetry factors in the preburning season were 0.66 at 1020 nm and 0.61 at 440 nm but decreased to 0.53 at 1020 nm and remained unchanged at 0.61 at 440 nm on average during the burning season. Large daily variations in these numbers were observed, however. Further analysis of the retrieved phase function, computation of the hemispherical backscatter fraction (beta), and the radiative significance is discussed by *Kaufman and Holben* [this issue].

Precipitable water was shown to increase from a season low in late June through July to near wet season values in late September and early October. The increase ranged from approximately 50 to 100% of the dry season minimum. This pattern held for all stations in the southern Amazon basin and was particularly evident in Cuiaba. Average temperatures at the surface for the period increased only 2°C. Although relative humidity was not measured, the implication is that it increased during this period, which corresponds to the time of most intense aerosol emissions from biomass burning. Despite this, there has been no clear difference in size distributions, asymmetry factors, or wavelength exponents between early burning season and late burning season observations. This would suggest that there is no observable growth in the aerosol size even with the increase in available moisture, and thus the Pw impact on optical properties of the aerosols is minor. Furthermore, with respect to radiational impacts, the aerosol-Pw interaction is minor compared to the direct impacts of aerosol scattering and absorption and by water vapor absorption separately. Field campaigns are needed to verify this conclusion, and a paper will follow to address the direct effect on the clear sky radiation balance.

Acknowledgments. Thanks to Diane Wickland and Tony Janetos for their NASA Headquarters support. We wish to thank Wayne Newcomb for his invaluable technical support. A special thanks to the many site managers in Brazil that have worked hard under difficult conditions to collect these data the last 3 years. These include José Roberto Chagas in Cuiaba, Bento da Silva Barros in Brasilia and during the Rondonia field campaign to Jamari, Arilon in Porto Nacional, Santurnino in Alta Floresta, Hugo in Santarem, Marcio in Jamari, Valeriano in Tucurui, Levi in Ji-Parana, and Benjamine of IBAMA in Ariquemas. Thanks also to Braulio Dias, formerly of IBAMA and IBGE, for organizing the instruments in Brasilia and Rondonia. Yoram Kaufman's encouragement, prodding, and suggestions throughout the development of the Brazil network have greatly helped to move the project forward. We would like to acknowledge the assistance of John Reagan for instrument evaluation and calibration and Didier Tanré for helping to develop the network.

References

Artaxo, P., and C. Orsini, The emission of the aerosol by plants revealed by three receptor models, in *Aerosols: Formation and Reactivity*, edited by G. Israel, pp. 148-151, Pergamon, New York, 1986.

Artaxo, P., H. Storms, F. Bruynseels, R. Van Grieken, and W. Maenhaut, Composition and sources of aerosols from the Amazon Basin, *J. Geophys. Res.*, *93*, 1605-1615, 1988.

Artaxo, P., W. Maenhaut, H. Storms, and R. Van Grieken, Aerosol characteristics and sources for the Amazon for the Amazon Basin during the wet season, *J. Geophys. Res.*, *95*, 16971-16985, 1990.

Artaxo, P., F. Gerab, and M.L.C. Rabello, Elemental composition of aerosol particles from two background monitoring stations in the Amazon Basin, *Nucl. Instrum. Methods Phys. Res., Section B75*, 277-281, 1993.

Artaxo, P., F. Gerab, M.A. Yamasoe, and J.V. Martins, Fine mode aerosol composition at three long-term atmospheric monitoring sites in the Amazon Basin, *J. Geophys. Res.*, *99*, 22, 857-22868, 1994.

Cachier, H., P. Buat-Menard, M. Fontugne, and J. Rancher, Source terms and source strengths of the carbonaceous aerosol in the tropics, *J. Atmos. Chem.*, 3, 469-489, 1985.

Charlson, R.J., S.E. Schwartz, J. M. Hales, R.D. Cess, J.A. Coakley Jr., J.E. Hansen, and D.J. Hofmann, Climate forcing by anthropogenic aerosols, *Science*, *255*, 423-430, 1992.

Crutzen, P.J., and M.O. Andreae, Biomass burning in the tropics: Impact on atmospheric chemistry and biogeochemical cycles, *Science*, *250*, 1669-1678, 1990.

Dutton, E.G., Aerosol optical depth measurements from four NOAA/CMDL monitoring sites, in *Trends '93: A Compendium of Data on Global Change*, edited by T.A. Boden, D.P. Kaiser, R.J. Sepanski, and F.W. Stoss, rep. *ORNL/CDIAC-65.*, pp. 484-494, Carbon Dioxide Inf. Analysis Cent., Oak Ridge Natl. Lab., Oak Ridge, Tenn., 1994.

Hansen, J.E., and A.A. Lacis, Sun and dust versus greenhouse gases: An assessment of their relative roles in global climate change, *Nature*, *346*, 713-719, 1990.

Harriss, R.C., et al., The Amazon Boundary Layer Experiment: Wet season 1987, *J. Geophys. Res.*, *95*, 16721-16736, 1990.

Holben, B.N., Y.J. Kaufman, A. Setzer, D. Tanre, and D.E. Ward, Optical properties of aerosol from biomass burning in the tropics, BASE-A, in *Global Biomass Burning*, pp. 403-411, MIT Press, Cambridge, Mass., 1991.

Holben, B.N., et al., Automatic sun and sky scanning radiometer system for network aerosol monitoring, *Remote Sens. Environ.*, in press 1996.

Kaufman, Y.J., A. Setzer, D. Ward., D. Tanré, B.N. Holben, P. Menzel, M.C. Pereira, and R. Rasmussen, Biomass burning airborne and spaceborne experiment in the Amazonas (BASE-A), *J. Geophy. Res.*, *97*, 14581-14599, 1992.

Kaufman, Y.J., and B.N. Holben, Hemispherical backscattering by biomass burning and sulfate particles derived from sky measurements, *J. Geophys. Res.*, this issue.

Lawson, D. R., and J.W. Winchester, Atmospheric sulfur aerosol concentrations and characteristics from the South American continent, *Science*, *205*, 1267-1269, 1979.

Nakajima, T., M. Tanaka, and T. Yamauchi, Retrieval of the optical properties of aerosols from aureole and extinction data, *Appl. Opt.*, *22*, 2951-2959, 1983.

Nakajima, T., T. Takamura, M. Yamano, M. Shiobara, T. Yamauchi, R. Goto, and K. Murai, Consistency of aerosol size distributions inferred from measurements of solar radiation and aerosols, *J. Meteorol. Soc. Jpn.*, *64*, 765-776, 1986.

Nakajima, T., T. Glauco, R. Rao, P. Boi, Y. Kaufman, and B. Holben, Use of sky brightness measurements from ground for remote sensing of particulate polyispersions, *Appl. Opt.*, *35*, 2672-2686, 1996.

Nimer, E., *Climatologia do Brasil*, Fundacao Instituto Brasileiro de Geografia e Estatistica, (IBGE), (2nd ed.), 421 pp. Rio de Janeiro, 1989.

Penner, J.E., R. Dickinson, and C. O'Neill, Effects of aerosol from biomass burning on the global radiation budget, *Science*, *256*, 1432-1434, 1992.

Penner, J.E., R. J. Charlson, J.M. Hales, N.S. Laulainen, R. Leifer, T. Novakov, J. Ogren, L.F. Radke, S.E. Schwartz, and L. Travis, Quantifying and minimizing uncertainty of climate forcing by anthropogenic aerosols, *Bull. Am. Meteorol. Soc.*, *75*(3), 375-399, 1994.

Prins, E.M., and Menzel, W.P., Geostationary satellite detection of biomass burning in South America, *Int. J. Remote Sensing.*, *13*(15), 2783-2799, 1992.

Prins, E.M., and W.P. Menzel, Trends in South American biomass burning detected with the GOES visible infrared spin scan radiometer atmospheric sounder from 1983 to 1991, *J. Geophys. Res.*, *99*, 16719-16735, 1994.

Remer, L.A., Y. Kaufman, and B. Holben, Comparison of smoke aerosol and urban/industrial aerosol optical properties, paper presented at the Chapman Conference on Biomass Burning and Global Changes Am. Geophys. Union, Williamsburg, Va., March 13-17, 1995.

Rosen, J.M., N.T. Kjome, R.L. McKenzie, and J.B. Liley, Decay of Mount Pinatubo aerosol and midlatitudes in the northern and southern hemispheres, *J. Geophys. Res.*, *99*, 25733-25739, 1994.

Russell, P.B., et al., Pinatubo and pre-Pinatubo optical-depth spectra: Mauna Loa measurements, somparisons, inferred particle size distributions, radiative effects, and relationship to lidar data, *J. Geophys. Res.*, *98*, 22969-22985, 1993.

Setzer, A., and M.C. Pereira, Amazonia biomass burning in 1987 and an estimate of their tropospheric emissions, *Ambio*, *20*, 19-22, 1991.

Skole, D., and C. Tucker, Tropical deforestation and habitat fragmentation in the Amazon: Satellite Data from 1978 to 1988, *Science*, *260*, 1905-1909, 1993.

T.F. Eck, Huges STX Corporation, Code 923, NASA GSFC, Greenbelt, MD 20771. (e-mail: teck@LTPsun.gsfc.nasa.gov)

B.N. Holben, NASA Goddard Space Flight Center, Code 923, Greenbelt, MD 20771. (e-mail: brent@Kratmos.gsfc.nasa.gov)

A.Pereira and A. Setzer, Instituto de Pesquisas Espaciais, Sao José dos Campos, San Paulo, Brazil. (e-mail: alfredo@ltid.inpe.br; asetzer@ltid.inpe.br)

I.Slutsker, Science Systems and Applications Inc., Code 923, NASA GSFC, Greenbelt, MD 20771. (e-mail: ilya@kratmos.gsfc.nasa.gov)

(Received July 10, 1995; revised March 11, 1996; accepted March 11, 1996.)